

# Synthesis and Evaluation of Small Molecule Inhibitors of the Androgen Receptor N-Terminal Domain

Martyn C. Henry,<sup>||</sup> Christopher M. Riley,<sup>||</sup> Irene Hunter, Jessica M. L. Elwood, J. Daniel Lopez-Fernandez, Laura Minty, Diane M. Coe, Iain J. McEwan,<sup>\*</sup> and Craig Jamieson<sup>\*</sup>



Cite This: *ACS Med. Chem. Lett.* 2023, 14, 1800–1806



Read Online

ACCESS |

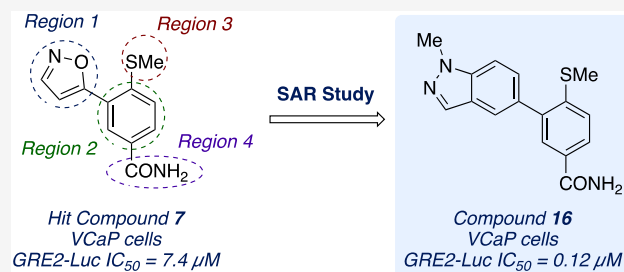
Metrics & More

Article Recommendations

Supporting Information

**ABSTRACT:** The androgen receptor (AR) is central to prostate cancer pathogenesis and has been extensively validated as a drug target. However, small-molecule anti-androgen therapies remain limited due to resistance and will eventually fail to suppress tumor growth, resulting in progression to castration-resistant prostate cancer (CRPC). The intrinsically disordered N-terminal domain (NTD) is crucial for AR transactivation and has been investigated as a suitable target in the presence of ligand binding domain mutations. A screening campaign identified biaryl isoxazole compound **7** as a weak inhibitor of the AR NTD. A library of biaryl analogues were synthesized, and their biological activities were assessed in a VCaP cell-based luciferase reporter gene assay. A structure–activity relationship (SAR) study revealed that indazole analogue **16** exhibited increased potency and favorable physicochemical properties with a benchmarked pharmacokinetic profile, providing a suitable starting point for further optimization of **16** as a CRPC therapeutic in the presence of AR mutations.

**KEYWORDS:** Prostate cancer, Androgen receptor, Intrinsically disordered protein



Prostate cancer remains the second most common cancer, with one in eight men receiving a diagnosis in their lifetime and almost 400,000 deaths worldwide in 2020 alone.<sup>1</sup> Despite significant advances in localized prostate cancer therapies, around 20–30% of patients will subsequently present with advanced and metastatic forms of the disease and will require systemic treatment.<sup>2–4</sup> While effective at inducing remission and offering a relief from symptoms, treatments such as androgen deprivation therapy (ADT) ultimately only slow the course of the disease before almost inevitable progression to castration-resistant prostate cancer (CRPC), which is associated with a poor prognosis.<sup>5,6</sup> Central to prostate cancer pathogenesis is the nuclear androgen receptor (AR), a 110 kDa transcription factor which is primarily responsible for androgen-mediated regulation of gene expression.<sup>7</sup> In common with all nuclear receptors, the AR protein consists of the ligand-binding domain (LBD), in which the ligand binding pocket (LBP) is located; the DNA-binding domain (DBD); the N-terminal domain (NTD); and a hinge region which connects the LBD with the DBD. Due to the critical role of the AR protein in the progression of prostate cancer, AR antagonists that compete with androgens for binding in the LBP are used clinically and have traditionally been the primary focus of drug discovery campaigns.<sup>8–10</sup> In this regard, the second-generation nonsteroidal anti-androgens (NSAAs) enzalutamide (**1**), apalutamide (**2**), and darolutamide (**3**) have all been approved within the past decade for the treatment of CRPC (Figure 1).<sup>11–13</sup> However, anti-androgen therapies will

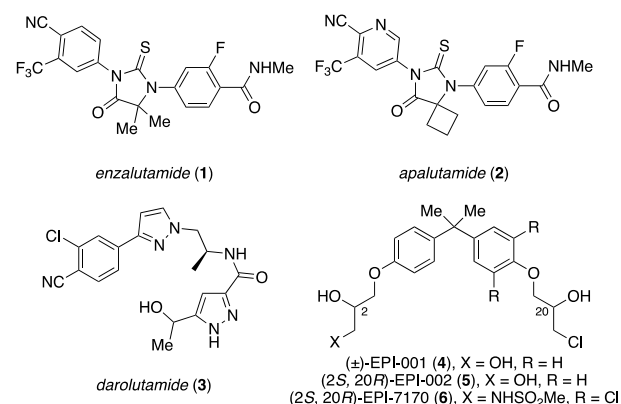


**Figure 1.** Clinically relevant nonsteroidal AR antagonists and recent AR-NTD AF1 binders.

eventually fail to suppress tumor growth due to a complex array of resistance mechanisms, which inevitably leads to reactivation of the AR signaling axis.<sup>14–19</sup> For this reason, alternative small-

**Received:** September 20, 2023

**Revised:** November 10, 2023

**Accepted:** November 13, 2023

**Published:** November 17, 2023



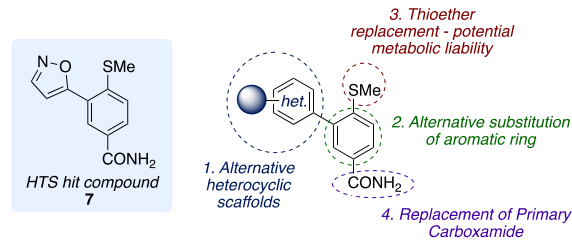
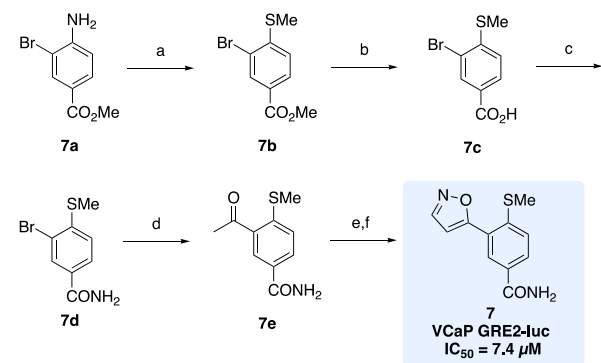
molecule CRPC therapies have been sought that do not rely on binding to the canonical LBD but instead target other domains of the AR.<sup>20–22</sup> It has been shown that the NTD is critical for the transactivation and function of AR, in which the modular activation function (AF-1) is of particular importance for gene expression and in facilitating protein–protein interactions.<sup>23,24</sup> However, due to the intrinsically disordered nature of this domain, it is not amenable to structure-based drug design and has therefore garnered less attention as a potential target for therapeutic intervention in the past.<sup>25</sup> Despite this, in the past decade, several small molecules have been developed which act on the AR via the disordered NTD.<sup>26–35</sup> For example, the EPI family of compounds,<sup>36–39</sup> including racemic EPI-001 (**4**), have been reported to block AR transcription via interaction with the AF-1 region of the AR-NTD, while other EPI analogues (EPI-002 (**5**) and EPI-7170 (**6**)) have been shown to induce conformation changes within the NTD and disrupt interactions between the AF1 and essential protein coactivators.<sup>40</sup> Furthermore, EPI-7386 (structure not disclosed) is currently in phase-1 clinical trials and has effectively demonstrated that AR NTD inhibitors could be potential therapeutics in the presence of LBD-driven resistance in the context of CPRC.<sup>41,42</sup>

Herein we report our work toward the design, synthesis, and biological evaluation of a novel series of biaryl small-molecule antagonists of the AR receptor NTD. Previous work within our laboratories identified compound **7** as a weak binder of AR splice variants (AR-vs) lacking the LBD using a high-throughput screen utilizing a functional cell-based assay developed in our group, with hits from this assay counterscreened for cytotoxicity and inhibition of luciferase activity to confirm specific activity.<sup>43</sup> In an effort to develop understanding of the structure–activity relationship (SAR) and identify more potent AR-NTD inhibitor analogues, we synthesized analogues of **7** focusing largely on changes to the LHS heterocyclic region, alternative substituents on the RHS aromatic ring, and replacement of the potentially metabolically labile thioether functional group (Figure 2a).

Our current work began with the validation of our screening-derived hit compound **7** in a cell-based reporter gene assay. This required the synthesis of compound **7** from readily available starting materials, which is shown in Figure 2b. Aniline **7a** was converted to the corresponding diazonium salt by treatment with sodium nitrite, which was followed by a Sandmeyer-type reaction with sodium methanethiolate that provided thioether **7b** in 86% yield. Hydrolysis of the ester group followed by amidation via *in situ* formation of the Vilsmier reagent afforded primary carboxamide **7d**. Palladium-catalyzed Heck reaction with ethyl vinyl ether gave the intermediate enol ether, which was hydrolyzed under acidic conditions to afford ketone **7e** in 43% yield. Finally, formylation of the  $\alpha$ -position of the carbonyl in the presence of sodium hydride followed by ring closure with hydroxylamine afforded isoxazole **7** in 25% yield over two steps. Compound **7** was then evaluated in our VCaP cell-based GRE2-luciferase reporter gene assay and was found to have an  $IC_{50}$  of 7.4  $\mu$ M.

For reference, the benchmark AR antagonist enzalutamide (**1**) and EPI-001 (**4**) were also examined for their effect against GRE2-luciferase activity in our hands (Figure 1). In this assay, enzalutamide was very potent, with an  $IC_{50}$  of 0.34  $\mu$ M, while EPI-001 had an  $IC_{50}$  of 37.4  $\mu$ M.

As shown in Figure 2a, the four main regions of the template were targeted for further SAR study. In our initial investigations into modifications of the LHS region, the biaryl C–C bond was used as a linchpin disconnection, with alternative heterocyclic

a) Screening-derived hit **7** and regions of planned structural modificationsb) Synthesis of screening-derived hit **7**

**Figure 2.** Proposed structural modifications and synthesis of initial HTS hit compound **7**. Reagents and conditions: (a)  $\text{NaNO}_2$ , 1 M HCl, rt, 1 h, then NaSMe, rt, 2 h, 86%; (b) 4 M NaOH, THF/EtOH (1:1), rt, 16 h, quant.; (c)  $(\text{COCl})_2$ , DMF, THF, rt, 1 h, then  $\text{NH}_4\text{OH}$ , 0 °C, 2 h, 74%; (d) ethyl vinyl ether, Pd(dppf) $\text{Cl}_2 \cdot \text{CH}_2\text{Cl}_2$ ,  $\text{K}_2\text{CO}_3$ , DMF/ $\text{H}_2\text{O}$  (9:1), 90 °C, 64 h, then 2 M HCl, rt, 0.5 h, 43%; (e) NaH, EtOCHO, rt, 24 h; (f)  $\text{H}_2\text{NOH} \cdot \text{HCl}$ , EtOH, 85 °C, 1 h, 25% over two steps.

groups being introduced via Suzuki–Miyaura cross-coupling with aryl bromide **7d** and a range of boronic acids under thermal or microwave conditions (Table 1; see the Supporting Information for further details). Compound **8** with an unfunctionalized phenyl ring was inactive in our assay.

Following this, the LHS region was explored via the introduction of smaller, five-membered heterocyclic motifs. Thiophene **9** showed robust activity ( $IC_{50}$  = 0.60  $\mu$ M), while dimethylisooxazole **10** was weakly active ( $IC_{50}$  = 4.7  $\mu$ M) and pyrrole **11** retained no activity. Next, benzannulated heterocycles bearing hydrogen-bond donors (HBDs) were examined. Indazole **12** showed good activity, with an  $IC_{50}$  of 0.70  $\mu$ M, while indole **13** displayed a 10-fold decrease in activity ( $IC_{50}$  = 10.3  $\mu$ M). Interestingly, indazole **14** featuring different connectivity compared with analogue **12**, such that the HBD is oriented in a different direction, was less potent ( $IC_{50}$  = 2.2  $\mu$ M). Activity was recovered with imidazole **15**, which displayed an  $IC_{50}$  of 0.92  $\mu$ M. Removing the HBD from the RHS heterocycle by blocking the free NH group of indazole **12** with a methyl substituent gave compound **16**, which exhibited excellent potency ( $IC_{50}$  = 0.12  $\mu$ M). This represents a 60-fold increase in potency over our initial hit compound **7** and compares favorably with enzalutamide ( $IC_{50}$  = 0.34  $\mu$ M). Deletion of a nitrogen atom resulted in approximately similar potency in *N*-methylindole **17** ( $IC_{50}$  = 0.09  $\mu$ M). Imidazopyridine **18** and oxindole **19** were tested; however, both displayed no activity. Quinoline **20** and isoquinoline **21** were active, both with an  $IC_{50}$  of 0.80  $\mu$ M, demonstrating that the position of the nitrogen atom has no effect on the activity. However, deleting the aryl ring resulted in a loss of activity of pyridine analogues **22** and **23**. The addition of a nitrogen atom in pyrimidine analogue

**Table 1. Region 1 Investigations into Alternative RHS Heterocyclic Scaffolds<sup>a</sup>**

Compound	R <sub>1</sub>	IC <sub>50</sub> (μM)	Compound	R <sub>1</sub>	IC <sub>50</sub> (μM)
8		>30	21		0.8
9		0.60	22		>30
10		4.7	23		>30
11		>30	24		0.27
12		0.70	25		0.60
13		10.3	26		>30
14		2.2	27		>30
15		0.92	28		>30
16		0.12	29		0.76
17		0.09	30		>30
18		>30	31		>30
19		>30	32		>30
20		0.8	33		0.12

<sup>a</sup>Conditions: (A) XPhos-Pd-G2 (5 mol %), K<sub>3</sub>PO<sub>4</sub>, toluene/water (9:1), 90 °C, 16 h; (B) Pd(PPh<sub>3</sub>)<sub>4</sub> (10 mol %), K<sub>3</sub>PO<sub>4</sub>, DMF/water (9:1), 90 °C, 16 h; (C) Pd(PPh<sub>3</sub>)<sub>4</sub> (7.5 mol %), Cs<sub>2</sub>CO<sub>3</sub>, 1,4-dioxane/water (9:1), 120 °C, 20 min (see the Supporting Information).

24 resulted in recovery of activity with an IC<sub>50</sub> of 0.27 μM. Our attention next focused on more lipophilic benzannulated heterocycles such as benzo[*b*]furan 25, benzoxazole 26, and 2,3-dihydrobenzofuran 27. Of these compounds, only unsaturated benzo[*b*]furan 25 displayed activity (IC<sub>50</sub> = 0.60 μM). Activity was abolished in electron-rich acyclic ether analogue 28 but recovered to an extent with the incorporation of a fluorine

atom in analogue 29 (IC<sub>50</sub> = 0.76 μM). Increasing the electron density of the ring and increasing the number of HBDs via the replacement of a methoxy group with an aryl amine resulted in loss of activity in compound 30. We next examined fluorinated phenol isomers 31, 32, and 33. Interestingly, the position of the fluorine atom on the aromatic ring significantly influenced the bioactivity, as *ortho* and *meta* analogues 31 and 32 were inactive while *para* derivative 33 was potent (IC<sub>50</sub> = 0.12 μM).

Subsequently, in an effort to improve solubility and other physicochemical properties, a  $\pi$ -deficient pyridine ring was introduced into our scaffold in analogues 34–37 (Table 2). It is

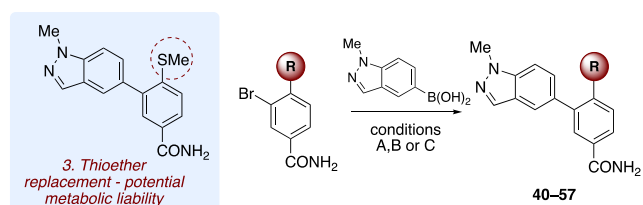
**Table 2. Region 2 Investigations into Alternative Substitutions of the LHS Aromatic Ring**

compound	substitution	IC <sub>50</sub> (μM)
34	R = SMe, X = N	>30
35	R = SBn, X = N	>30
36	R = H, X = N	>30
37	R = OMe, X = N	>30
38	R = SMe, X = CF	0.24
39	R = H, X = C-SMe	>30

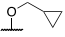
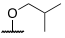
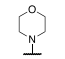
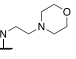
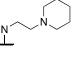
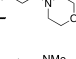

clear from matched molecular pairs 34 and 16 that the pyridine ring is not tolerated on the RHS, resulting in a loss of activity, perhaps due to unfavorable conformation changes or a decrease in electron density. Substitution of a hydrogen atom for a fluorine atom at the *ortho* position with respect to the thioether in compound 38 gave activity (IC<sub>50</sub> = 0.24 μM) similar to that of compound 16. Moving the thioether group around the ring to furnish *meta* substitution relative to the biaryl C–C bond resulted in an inactive compound (39).

Replacement of the methyl thioether functionality was next investigated, as it was reasoned that this could be a potential metabolic liability (Table 3). This required *de novo* synthesis from prefunctionalized starting materials (see the Supporting Information for experimental details). For example, ether starting materials were prepared by O-alkylation, while nitrogen functionality was introduced via nucleophilic aromatic substitution with the desired amine. Compounds 40–57 were then delivered by subjecting these starting materials to a palladium-catalyzed Suzuki–Miyaura cross-coupling with methylindazole boronic acid, as detailed previously.

First, replacement of the methyl group with a bulkier, more lipophilic benzyl group resulted in moderately potent compound 40 (IC<sub>50</sub> = 2.2 μM), while substitution of the thioether with alkyl functionality (methyl 41 and ethyl 42) resulted in loss of activity. Similarly, no bioactivity was observed for compound 43 after removal of the thioether and replacement with a hydrogen atom. While fluorinated analogue 44 was inactive, compound 45 bearing a trifluoromethyl group was weakly active, with an IC<sub>50</sub> of 8.6 μM. Attempts to introduce ether functionality resulted in complete loss of activity, with methyl ether 46, benzyl ether 47, and trifluoromethyl ether 48 all displaying IC<sub>50</sub> > 30 μM. Furthermore, a similar lack of activity was observed with free phenol derivative 49, while

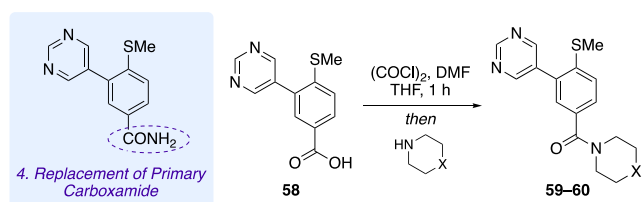
**Table 3. Region 3 Investigations into Potential Replacement of the Thioether Functional Group**


3. Thioether replacement - potential metabolic liability

Compound	R <sub>1</sub>	IC <sub>50</sub> (μM)	Compound	R <sub>1</sub>	IC <sub>50</sub> (μM)
40	SBn	2.2	49	OH	>30
41	Me	>30	50		>30
42	Et	>30	51		>30
43	H	>30	52	NHBn	0.94
44	F	>30	53		>30
45	CF <sub>3</sub>	8.6	54		>30
46	OMe	>30	55		>30
47	OBn	>30	56		0.8
48	OCF <sub>3</sub>	>30	57		>30

bulkier ether analogues **50** and **51** were all inactive in our assay. Changing the C–O linkage to a C–N bond in compound **52** resulted in modest activity, with an IC<sub>50</sub> of 0.94 μM. Alternative N-linked analogues were synthesized, including cyclic morpholine compound **53** and acyclic derivatives **54**–**57**. Only analogue **56** featuring a morpholine ring attached to the LHS aryl ring via a linear propyl amine chain was active in the assay, with an IC<sub>50</sub> of 0.80 μM.

For reasons of synthetic tractability, molecular matched pairs of pyrimidine analogue **24** were investigated where the primary carboxamide was replaced with tertiary amides via coupling of carboxylic acid **58** with cyclic secondary amines (Table 4). In the VCaP GRE2-luciferase assay, carboxylic acid **58** was active, with an IC<sub>50</sub> value of 0.12 μM, while tertiary amides **59** and **60**

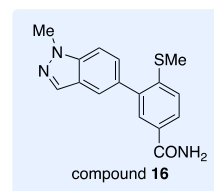
**Table 4. Region 4 Investigations into Potential Replacement of the Primary Carboxamide**


4. Replacement of Primary Carboxamide

compound	substitution	IC <sub>50</sub> (μM)
58	CO <sub>2</sub> H	0.12
59	X = CH <sub>2</sub>	0.13
60	X = O	0.26

exhibited IC<sub>50</sub> values of 0.13 and 0.26 μM, respectively. Compounds **59** and **60** displayed comparable potency to matched pair **24**, which suggests that the HBD capabilities of the primary amide are not crucial for binding to the AR.

During the SAR investigation of the core scaffold, control of lipophilicity was maintained with the aim of keeping this parameter in the desired Lipinski-type space. A ligand lipophilicity (LLE) plot showing the effects of changes by region revealed no significant correlation between cellular potency and cLogP (see the Supporting Information for further information). The *in vitro* activity (IC<sub>50</sub> = 0.12 μM) and favorable physicochemical properties placed methylindazole **16** within lead-like chemical space (Table 5). The lipophilicity

**Table 5. Physicochemical Properties and In Vitro Pharmacokinetic Profile of Compound 16**


Physicochemical Properties

MW	= 297.4
cLogP	= 2.3
TPSA	= 86
iPFI	= 5.3
HBD	= 2
HBA	= 4
LE	= 0.33
LLE	= 4.7

compound **16**

VCaP GRE2-luciferase IC <sub>50</sub>	0.12 μM
solubility	2.6 μM
Caco2 permeability P <sub>app</sub> A2B (nm/s); P <sub>app</sub> B2A (nm/s)	331; 394
Caco2 efflux ratio	1.2
HLM CL <sub>int</sub> (μL min <sup>-1</sup> mg <sup>-1</sup> )	25.6
HLM t <sub>1/2</sub> (min)	54
plasma fraction unbound (mouse)	6.9%
CYP IC <sub>50</sub> (3A4; 2D6)	>25 μM
hERG IC <sub>50</sub>	>10 μM

(cLogP = 2.3), topological polar surface area (TPSA = 86), and numbers of HBDs (2) and hydrogen bond acceptors (HBAs) (4) were all within the desired property space associated with lead assets.<sup>44</sup> The intrinsic property forecast index (iPFI), a metric proposed by Young and co-workers,<sup>45</sup> is the sum of cLogP and the aromatic ring count, which is a predictor of important considerations such as solubility and off-target effects and should be kept <7. The iPFI of compound **16** is in the acceptable range, with a value of 5.3. Moreover, compound **16** has a ligand efficiency of 0.33 and a ligand-lipophilic efficiency of 4.7.

Having demonstrated robust *in vitro* and physicochemical properties, we next sought to further probe the pharmacology of emerging lead compound **16**. To this end, AR-v splice variant activity was determined through transfection of PC3 cells with an AR<sub>NTD-DBD</sub> expression plasmid and a GRE2-luciferase reporter gene (Figure 3).<sup>43</sup> This construct retains the constitutively active NTD/DBD core; however, it is insensitive to LBD antagonists such as enzalutamide. Compound **16** shows 35% inhibition of AR-v activity at 10 μM, whereas enzalutamide is not active in this assay. In addition to this, we evaluated hormone-dependent expression of prostate-specific antigen (PSA) in VCaP cells (see the Supporting Information). This showed a similar level of inhibition (34%), confirming pathway-relevant pharmacological effects.

We next explored the potential developability of this compound as a potent AR inhibitor with an investigation of the *in vitro* pharmacokinetic properties of **16** (Table 5). Compound **16** exhibited a moderate thermodynamic aqueous

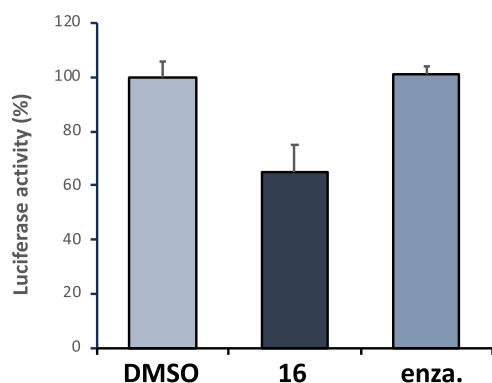


**Figure 3.** Small-molecule inhibition of androgen receptor transcriptional activity of compound **16** and enzalutamide (enza.).

solubility of 2.6  $\mu\text{M}$  and good Caco2 cell permeability (apical to basolateral of 33.1 nm/s and basolateral to apical of 39.4 nm/s), with an efflux ratio of 1.2. Furthermore, compound **16** displayed promising intrinsic clearance ( $CL_{\text{int}}$ ) in human liver microsomes and a half-life of 54 min. The plasma protein binding of **16** was determined and showed a free fraction of 6.9%. The potential for drug–drug interactions was next investigated, and no inhibition of CYP450 was observed (with both 3A4 and 2D6 isoforms), while no hERG channel inhibition was observed via a Q-patch clamp assay.

Encouraged by the promising *in vitro* profile, compound **16** was advanced, and a pharmacokinetic (PK) profile was obtained in male CD-1 mice (Table 6). When compound **16** was

**Table 6.** *In Vivo* PK Profile of Compound **16** in Mouse ( $n = 3$ )

PK parameters	iv (1 mg/kg)	po (10 mg/kg)
$t_{1/2}$ (h)	0.29	4
$T_{\text{max}}$	n/a	0.25
CL ( $\text{mL min}^{-1} \text{kg}^{-1}$ )	126	n/a
$C_{\text{max}}$ (ng/mL)	432	195
$AUC_{0-t}$ (h·ng/mL)	131	173
$AUC_{0-\infty}$ (h·ng/mL)	132	208
$V_{\text{ss, obs}}$ (L/kg)	1.38	n/a
$F$ (%)	n/a	16

administered intravenously (iv) at 1 mg/kg, a short half-life ( $t_{1/2}$ ) of 0.29 h was observed along with a high clearance of 126  $\text{mL min}^{-1} \text{kg}^{-1}$ . The maximum plasma concentration ( $C_{\text{max}}$ ) was 432 ng/mL, while the area under the curve (AUC) was 131 h·ng/mL (as can be seen in the  $C_{\text{max}}$  versus time profile in Figure 4). Following an oral dose (p.o.) of compound **16** at 10 mg/kg, a mean half-life of 4 h was observed along with adequate plasma exposure ( $C_{\text{max}} = 195 \text{ ng/mL}$ ) and measurable exposure (AUC = 173 h·ng/mL) with an oral bioavailability ( $F$ ) of 16%, suggesting that target engagement may be difficult to achieve when considering the potency and exposure data.

In summary, after identification and validation of initial hit **7** as a weak binder of the AR NTD, 50 analogues were synthesized to explore the SAR and optimize potency. Investigations into region 1 revealed that several benzannulated N-heterocycles were tolerated and had elevated activity compared to the initial hit. In particular, the *N*-methylindazole analogue **16** showed a 60-fold increase in potency over the progenitor compound **7**. Furthermore, compound **16** compared favorably in terms of potency to the clinically deployed AR antagonist enzalutamide

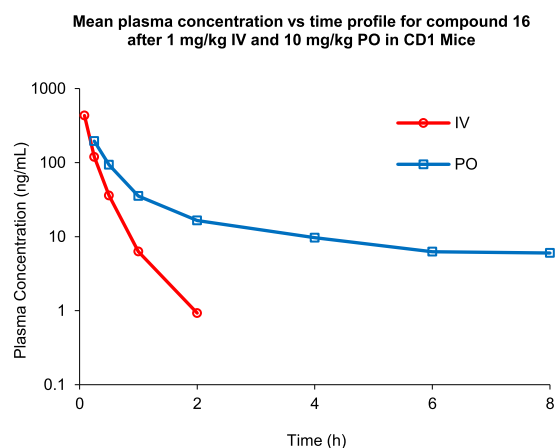


**Figure 4.**  $C_{\text{max}}$  versus time profile for compound **16**.

( $IC_{50} = 0.34 \mu\text{M}$ ) and was more potent than known AR-NTD AF1 binder EPI-001 ( $IC_{50} = 37.4 \mu\text{M}$ ) under the assay conditions. Together, the excellent potency, favorable physicochemical properties, and benchmarked pharmacokinetic profile offer a starting point for the further optimization of compound **16** as a tool compound to investigate the pharmacology and engagement of the AR NTD. Further optimization of this emerging chemical equity is underway in our laboratories, focusing on tuning the metabolic profile to attain exposure consistent with target engagement as well as biophysical studies of the interaction with the AR-NTD, and will be reported in due course.

## ASSOCIATED CONTENT

### Supporting Information

The Supporting Information is available free of charge at <https://pubs.acs.org/doi/10.1021/acsmchemlett.3c00426>.

Preparative details of all compounds and requisite intermediates, associated spectral data, and bioassay procedures (PDF)

## AUTHOR INFORMATION

### Corresponding Authors

**Craig Jamieson** – Department of Pure and Applied Chemistry, University of Strathclyde, Glasgow G1 1XL, U.K.;

[orcid.org/0000-0002-6567-8272](https://orcid.org/0000-0002-6567-8272);

Email: [craig.jamieson@strath.ac.uk](mailto:craig.jamieson@strath.ac.uk)

**Iain J. McEwan** – Institute of Medical Sciences, University of Aberdeen, Aberdeen AB25 2ZD, U.K.; Email: [iain.mcewan@abdn.ac.uk](mailto:iain.mcewan@abdn.ac.uk)

### Authors

**Martyn C. Henry** – Department of Pure and Applied Chemistry, University of Strathclyde, Glasgow G1 1XL, U.K.

**Christopher M. Riley** – Department of Pure and Applied Chemistry, University of Strathclyde, Glasgow G1 1XL, U.K.

**Irene Hunter** – Institute of Medical Sciences, University of Aberdeen, Aberdeen AB25 2ZD, U.K.

**Jessica M. L. Elwood** – Department of Pure and Applied Chemistry, University of Strathclyde, Glasgow G1 1XL, U.K.

**J. Daniel Lopez-Fernandez** – Department of Pure and Applied Chemistry, University of Strathclyde, Glasgow G1 1XL, U.K.

**Laura Minty** – Department of Pure and Applied Chemistry, University of Strathclyde, Glasgow G1 1XL, U.K.

Diane M. Coe – Medicine Design, GlaxoSmithKline R&D Ltd, Stevenage, Hertfordshire SG1 2NY, U.K.

Complete contact information is available at:  
<https://pubs.acs.org/10.1021/acsmedchemlett.3c00426>

### Author Contributions

<sup>†</sup>M.C.H. and C.M.R. contributed equally. All of the authors approved the final version of the manuscript.

### Funding

We thank the Medical Research Council (MR/T02559/X), Prostate Cancer Research (IH), and GlaxoSmithKline for financial support of this work.

### Notes

The authors declare no competing financial interest.

### ACKNOWLEDGMENTS

We thank Craig Irving for his assistance with NMR spectroscopy and Pat Keating, Dr. Jessica Bame, and Dr. Graeme Anderson for their assistance with HRMS.

### ABBREVIATIONS

ADT, androgen deprivation therapy; AF-1, activation function-1; AR, androgen receptor; AUC, area under the curve;  $Cl_{int}$ , intrinsic clearance; CRPC, castration-resistant prostate cancer; CYP, cytochrome P; DBD, DNA binding domain; HBA, hydrogen-bond acceptor; HBD, hydrogen-bond donor; LBD, ligand binding domain; LBP, ligand binding pocket; NSAA, nonsteroidal anti-androgen; NTD, N-terminal domain; iPFI, intrinsic property forecast index; SAR, structure–activity relationship; TPSA, topological polar surface area.

### REFERENCES

- (1) *Global Cancer Observatory*. World Health Organization, 2020. <https://gco.iarc.fr/>.
- (2) *Drug Management of Prostate Cancer*; Figg, W. D., Chau, C. H., Small, E. J., Eds.; Springer, 2010.
- (3) Imamura, Y.; Sadar, M. D. Androgen Receptor Targeted Therapies in Castration-resistant Prostate Cancer: Bench to Clinic. *Int. J. Urol.* **2016**, *23*, 654–665.
- (4) Siegel, R. L.; Miller, K. D.; Jemal, A. Cancer statistics. *CA Cancer J. Clin.* **2019**, *69*, 7–34.
- (5) Pienta, K. J.; Bradley, D. Mechanisms underlying the development of androgen-independent prostate cancer. *Clin. Cancer Res.* **2006**, *12*, 1665–1671.
- (6) Harris, W. P.; Mostaghel, E. A.; Nelson, P. S.; Montgomery, B. Androgen Deprivation Therapy: Progress in Understanding Mechanisms of Resistance and Optimizing Androgen Depletion. *Nat. Clin. Pract. Urol.* **2009**, *6*, 76–85.
- (7) Tan, M. H. E.; Li, J.; Xu, H. E.; Melcher, K.; Yong, E.-L. Androgen receptor: structure, role in prostate cancer and drug discovery. *Acta Pharmacol. Sin.* **2015**, *36*, 3–23.
- (8) Helsen, C.; Van den Broeck, T.; Voet, A.; Prekovic, S.; Van Poppel, H.; Joniau, S.; Claessens, F. Androgen receptor antagonists for prostate cancer therapy. *Endocr. Relat. Cancer.* **2014**, *21*, T105–T118.
- (9) Crawford, E. D.; Schellhammer, P. F.; McLeod, D. G.; Moul, J. W.; Higano, C. S.; Shore, N.; Denis, L.; Iversen, P.; Eisenberger, M. A.; Labrie, F. Androgen Receptor Targeted Treatments of Prostate Cancer: 35 Years of Progress with Antiandrogens. *J. Urol.* **2018**, *200*, 956–966.
- (10) Estébanez-Perpiñá, E.; Bevan, C. L.; McEwan, I. J. Eighty Years of Targeting Androgen Receptor Activity in Prostate Cancer: The Fight Goes on. *Cancers* **2021**, *13*, 509.
- (11) Tran, C.; Ouk, S.; Clegg, N. J.; Chen, Y.; Watson, P. A.; Arora, V.; Wongvipat, J.; Smith-Jones, P. M.; Yoo, D.; Kwon, A.; Wasielewska, T.; Welsbie, D.; Chen, C. D.; Higano, C. S.; Beer, T. M.; Hung, D. T.; Scher, H. I.; Jung, M. E.; Sawyers, C. L. Development of a Second Generation Antiandrogen for Treatment of Advanced Prostate Cancer. *Science* **2009**, *324*, 787–790.
- (12) Dellis, A. E.; Papatsoris, A. G. Apalutamide: The Established and Emerging Roles in the Treatment of Advanced Prostate Cancer. *Expert Opin. Invest. Drugs.* **2018**, *27*, 553–559.
- (13) Moilanen, A.-M.; Riikonen, R.; Oksala, R.; Ravanti, L.; Aho, E.; Wohlfahrt, G.; Nykänen, P. S.; Törmäkangas, O. P.; Palvimo, J. J.; Kallio, P. J. Discovery of ODM-201, A New-Generation Androgen Receptor Inhibitor Targeting Resistance Mechanisms to Androgen Signalling-Directed Prostate Cancer Therapies. *Sci. Rep.* **2015**, *5*, 12007.
- (14) Chandrasekar, T.; Yang, J. C.; Gao, A. C.; Evans, C. P. Mechanisms of resistance in castration-resistant prostate cancer (CRPC). *Transl. Androl. Urol.* **2015**, *4*, 365–380.
- (15) Watson, P. A.; Arora, V. K.; Sawyers, C. L. Emerging mechanisms of resistance to androgen receptor inhibitors in prostate cancer. *Nat. Rev. Cancer* **2015**, *15*, 701–711.
- (16) Tilkki, D.; Schaeffer, E. M.; Evans, C. P. Understanding Mechanisms of Resistance in Metastatic Castration-resistant Prostate Cancer: The Role of the Androgen Receptor. *Eur. Urol. Focus* **2016**, *2*, 499–505.
- (17) Crona, D. J.; Whang, Y. E. Androgen Receptor-Dependent and -Independent Mechanisms Involved in Prostate Cancer Therapy Resistance. *Cancers* **2017**, *9*, 67.
- (18) Huang, Y.; Jiang, X.; Liang, X.; Jiang, G. Molecular and cellular mechanisms of castration-resistant prostate cancer. *Oncol. Lett.* **2018**, *15*, 6063–6076.
- (19) Schmidt, K. T.; Huitema, A. D. R.; Chau, C. H.; Figg, W. D. Resistance to Second-Generation Androgen Receptor Antagonists in Prostate Cancer. *Nat. Rev. Urol.* **2021**, *18*, 209–226.
- (20) Lallous, N.; Dalal, K.; Cherkasov, A.; Rennie, P. S. Targeting Alternative Sites on the Androgen Receptor to Treat Castration-Resistant Prostate Cancer. *Int. J. Mol. Sci.* **2013**, *14*, 12496–12519.
- (21) Elshan, N. G. R. D.; Rettig, M. B.; Jung, M. E. Molecules targeting the androgen receptor (AR) signalling axis beyond the AR-Ligand binding domain. *Med. Res. Rev.* **2019**, *39*, 910–960.
- (22) Riley, C. M.; Elwood, J. M. L.; Henry, M. C.; Hunter, I.; Lopez-Fernandez, J. D.; McEwan, I. J.; Jamieson, C. Current and Emerging Approaches to Noncompetitive AR inhibition. *Med. Res. Rev.* **2023**, *43*, 1701.
- (23) Jenster, G.; Van der Korput, H. A.; Trapman, J.; Brinkmann, A. O. Identification of Two Transcription Activation Units in the N-Terminal Domain of the Human Androgen Receptor. *J. Biol. Chem.* **1995**, *270*, 7341–7346.
- (24) Reid, J.; Kelly, S. M.; Watt, K.; Price, N. C.; McEwan, I. J. Conformational Analysis of the Androgen Receptor Amino-Terminal Domain Involved in Transactivation. Influence of Structure-Stabilizing Solutes and Protein-Protein Interactions. *J. Biol. Chem.* **2002**, *277*, 20079–20086.
- (25) McEwan, I. J. Intrinsic Disorder in the Androgen Receptor: Identification, Characterisation and Drugability. *Mol. Biosyst.* **2012**, *8*, 82–90.
- (26) Monaghan, A.; McEwan, I. A Sting in the Tail: the N-Terminal Domain of the Androgen Receptor as a Drug Target. *Asian J. Androl.* **2016**, *18*, 687–694.
- (27) Antonarakis, E. S.; Chandhasin, C.; Osbourne, E.; Luo, J.; Sadar, M. D.; Perabo, F. Targeting the N-Terminal Domain of the Androgen Receptor: A New Approach for the Treatment of Advanced Prostate Cancer. *Oncologist* **2016**, *21*, 1427–1435.
- (28) Hupe, M. C.; Offermann, A.; Perabo, F.; Chandhasin, C.; Perner, S.; Merseburger, A. S.; Cronauer, M. V. Inhibitors of the Androgen Receptor N-Terminal Domain: Therapies Targeting the Achilles' Heel of Various Androgen Receptor Molecules in Advanced Prostate Cancer. *Urology* **2018**, *57*, 148–154.
- (29) Sadar, M. D. Discovery of Drugs that Directly Target the Intrinsically Disordered Region of the Androgen Receptor. *Expert Opin. Drug Discovery* **2020**, *15*, 551–560.

- (30) Ji, Y.; Zhang, R.; Han, X.; Zhou, J. Targeting the N-Terminal Domain of the Androgen Receptor: The Effective Approach in Therapy of CRPC. *Eur. J. Med. Chem.* **2023**, *247*, 115077.
- (31) Li, H.; Hassona, M. D. H.; Lack, N. A.; Axerio-Cilies, P.; Leblanc, E.; Tavassoli, P.; Kanaan, N.; Frewin, K.; Singh, K.; Adomat, H.; Böhm, K. J.; Prinz, H.; Guns, E. T.; Rennie, P. S.; Cherkasov, A. Characterization of a New Class of Androgen Receptor Antagonists with Potential Therapeutic Application in Advanced Prostate Cancer. *Mol. Cancer Ther.* **2013**, *12*, 2425–2435.
- (32) Banuelos, C. A.; Lal, A.; Tien, A. H.; Shah, N.; Yang, Y. C.; Mawji, N. R.; Meimetis, L. G.; Park, J.; Kunzhong, J.; Andersen, R. J.; Sadar, M. D. Characterisation of Niphatenones that Inhibit Androgen Receptor N-Terminal Domain. *PLoS One* **2014**, *9*, No. e107991.
- (33) Banuelos, C. A.; Tavakoli, I.; Tien, A. H.; Caley, D. P.; Mawji, N. R.; Li, Z.; Wang, J.; Yang, Y. C.; Imamura, Y.; Yan, L.; Wen, J. G.; Andersen, R. J.; Sadar, M. D. Sintokamide A is a Novel Antagonist of Androgen Receptor that Uniquely Binds Activation Function-1 in its Amino-terminal Domain. *J. Biol. Chem.* **2016**, *291*, 22231–22243.
- (34) Peng, S.; Wang, J.; Chen, H.; Hu, P.; He, X.-L.; He, Y.; Wang, M.; Tang, W.; He, Q.; Wang, Y.-Y.; Xie, J.; Guo, D.; Ren, S.; Liu, M.; Qiu, W.-W.; Yi, Z. Regression of Castration-Resistant Prostate Cancer by a Novel Compound QW07 Targeting Androgen Receptor N-Terminal Domain. *Cell. Biol. Toxicol.* **2020**, *36*, 399–416.
- (35) Yang, Z.; Wang, D.; Johnson, J. K.; Pascal, L. E.; Takubo, K.; Avula, R.; Chakka, A. B.; Zhou, J.; Chen, W.; Zhong, M.; Song, Q.; Ding, H.; Wu, Z.; Chandran, U. R.; Maskrey, T. S.; Nelson, J. B.; Wipf, P.; Wang, Z. A Novel Small Molecule Targets Androgen Receptor and Its Splice Variants in Castration-Resistant Prostate Cancer. *Mol. Cancer Ther.* **2020**, *19*, 75–88.
- (36) Andersen, R. J.; Mawji, N. R.; Wang, J.; Wang, G.; Haile, S.; Myung, J.-K.; Watt, K.; Tam, T.; Yang, Y.-C.; Bañuelos, C. A.; Williams, D. E.; McEwan, I. J.; Wang, Y.; Sadar, M. D. Regression of Castrate-Recurrent Prostate Cancer by a Small-Molecule Inhibitor of the Amino-Terminus Domain of the Androgen Receptor. *Cancer Cell* **2010**, *17*, 535–546.
- (37) Myung, J.-K.; Bañuelos, C. A.; Fernandez, J. G.; Mawji, N. R.; Wang, J.; Tien, A. H.; Yang, Y. C.; Tavakoli, I.; Haile, S.; Watt, K.; McEwan, I. J.; Plymate, S.; Andersen, R. J.; Sadar, M. D. An Androgen Receptor N-Terminal Domain Antagonist for Treating Prostate Cancer. *J. Clin. Invest.* **2013**, *123*, 2948–2960.
- (38) Yang, Y. C.; Bañuelos, C. A.; Mawji, N. R.; Wang, J.; Kato, M.; Haile, S.; McEwan, I. J.; Plymate, S.; Sadar, M. D. Targeting Androgen Receptor Activation Function-1 with EPI to Overcome Resistance Mechanisms in Castration-Resistant Prostate Cancer. *Clin. Cancer Res.* **2016**, *22*, 4466–4477.
- (39) De Mol, E.; Fenwick, R. B.; Phang, C. T. W.; Buzón, V.; Szulc, E.; de la Fuente, A.; Escobedo, A.; Garcia, J.; Bertocini, C. W.; Estébanez-Perpiñá, E.; McEwan, I. J.; Riera, A.; Salvatella, X. EPI-001, A Compound Active against Castration-Resistant Prostate Cancer, Targets Transactivation Unit 5 of the Androgen Receptor. *ACS Chem. Biol.* **2016**, *11*, 2499–2505.
- (40) Zhu, J.; Salvatella, X.; Robustelli, P. Small Molecules Targeting the Disordered Transactivation Domain of the Androgen Receptor Induce the Formation of Collapsed Helical States. *Nat. Commun.* **2022**, *13*, 6390.
- (41) Le Moigne, R.; Bañuelos, C. A.; Mawji, N. R.; Tam, T.; Wang, J.; Jian, K.; Andersen, R. J.; Cesano, A.; Sadar, M. D.; Zhou, H.-J.; Virsik, P. IND candidate EPI-7386 as an N-Terminal Domain Androgen Receptor Inhibitor in Development for the Treatment of Prostate Cancer. *J. Clin. Oncol.* **2020**, *38*, 142.
- (42) Laccetti, A. L.; Chatta, G. S.; Iannotti, N.; Kyriakopoulos, C.; Villaluna, K.; Le Moigne, R.; Cesano, A. Phase 1/2 Study of EPI-7386 in Combination with Enzalutamide (enz) Compared with enz Alone in Subjects with Metastatic Castration-Resistant Prostate Cancer (mCRPC). *J. Clin. Oncol.* **2023**, *41*, 179–179.
- (43) Monaghan, A. E.; Porter, A.; Hunter, I.; Morrison, A.; McElroy, S. P.; McEwan, I. J. Development of a High-Throughput Screening Assay for Small-Molecule Inhibitors of Androgen Receptor Splice Variants. *Assay Drug Dev. Technol.* **2022**, *20*, 111–124.
- (44) Sander, T.; Freyss, J.; von Korff, M.; Rufener, C. DataWarrior: An Open-Source Program for Chemistry Aware Data Visualization and Analysis. *J. Chem. Inf. Model.* **2015**, *55*, 460–473.
- (45) Young, R. J.; Green, D. V. S.; Luscombe, C. N.; Hill, A. P. Getting Physical in Drug Discovery II: The Impact of Chromatographic Hydrophobicity Measurements and Aromaticity. *Drug Discovery Today* **2011**, *16*, 822–830.